

Temperature Control of Rubber Composites by Adaptive Multidimensional Taylor Network during Microwave Heating Process

Shanliang Zhu^{1, 2, 3}, Chengcheng Li¹, Yi Yang^{2, 3}, and Qingling Li^{1, *}

Abstract—Microwave technology has been widely used in rubber industry. In order to solve the problem of uneven temperature distribution, a novel control method of adaptive multi-dimensional Taylor network combined with Cuckoo Search is proposed in this paper. The adaptive multi-dimensional Taylor network control method is used to obtain the suitable output powers and phase difference under unknown system parameters. Cuckoo Search algorithm is utilized to optimize the whole situation and find the best fit input variables at sampling points. To verify the proposed control strategy, the dielectric permittivity of nitrile butadiene rubber composites is measured, and the control process is simulated based on measured values. The simulation results show that the proposed method can well control the temperature rising process with little difference between the average temperature and reference trajectory.

1. INTRODUCTION

In recent years, more and more importance has been attached to microwave energy due to its environmental protection and energy saving in rubber industry. Microwave heating technology has been used in preheating, rapid curing, vulcanization, and drying. Many previous studies have been reported [1–6]. For instance, Makul and Rattanadecho [1] proposed a new mathematical model for predicting temperature distribution inside the specimen during preheating natural rubber-compounding by using microwave energy. Chen et al. [4] experimentally studied the temperature distribution in the sheet rubber during microwave heating. They concluded that the temperature distribution in the rubber sheet is seriously uneven, and the highest temperature occurred in the center zone of rubber sheet. In fact, the problem of hot spots has always been one of the key problems of microwave heating research, which has become one of the major drawbacks for industrial application [7–11].

However, the research on temperature uniformity control method in microwave heating process is rarely reported due to its complex application environment [12–15]. Huang and Sites [12] developed a microwave heating system equipped with a proportional-integral-differential (PID) control device for in-package pasteurization of ready-to-eat meats. This control mechanism can improve the effect of the temperature control, but the temperature difference between the surface temperature and the reference is large. Akkari et al. [13] studied the problem of a global linearizing control algorithm for a multi-input-multi-output (MIMO) microwave thawing process. This method can control the defrosting time while preventing thermal runaway. However, the method requires a precise power distribution, which is difficult to achieve in practical applications. Li et al. [14] demonstrated the effectiveness of microwave heating control by the sliding mode neural network algorithm in two microwave sources under the assumption that the temperature of the surrounding medium was constant. However, higher medium

Received 4 February 2020, Accepted 27 April 2020, Scheduled 11 May 2020

* Corresponding author: Qingling Li (qustmaths@126.com).

¹ College of Electromechanical Engineering, Qingdao University of Science and Technology, Qingdao 266061, China. ² School of Mathematics and Physics, Qingdao University of Science and Technology, Qingdao 266061, China. ³ Research Institute for Mathematics and Interdisciplinary Sciences, Qingdao University of Science and Technology, Qingdao 266061, China.

temperature was not considered because the above assumption is not true in a higher temperature environment.

In recent years, a multi-dimensional Taylor network (MTN) has been used in the nonlinear system identification and control [16]. The approximation-based MTN control scheme has been proved to be an effective and reliable method for nonlinear system control [17–19]. Motivated from the above researches, a novel method of combining the adaptive MTN and Cuckoo Search algorithm is proposed to solve the problem of uneven temperature distribution during the microwave heating in this paper. The suitable input powers at sampling points are obtained by the proposed adaptive control law in the microwave heating control system. MTN is selected to identify the unknown functions in the system, and the MTN parameters are adjusted in an online manner. Cuckoo Search is utilized to optimize the whole situation and find the best fit inputs powers at those sampling points. In order to verify the proposed control strategy, a kind of nitrile butadiene rubber (NBR) composites is selected as microwave heating materials, and the temperature dependent dielectric properties are measured experimentally. The simulation results show that the difference between the average temperature of those sampling points and the reference trajectory is controlled well, and the uniform temperature rising process of the NBR sample can be realized. The main contributions of this paper are summarized as follows:

(i) For the first time, the MTN approach is utilized to the temperature control in microwave heating. A new adaptive MTN control algorithm combined with Cuckoo Search algorithm is designed, which effectively improves the uniformity of temperature field.

(ii) The proposed control strategy can solve the problem of temperature control during microwave heating process when the ambient temperature of the medium changes with the heating temperature of the medium. However, to the authors' knowledge, the existing results were obtained under the condition that the ambient temperature of the medium was constant.

2. HEAT TRANSFER MODEL

Considering a one-dimensional slab of the rubber material of thickness L exposed to uniform plane microwave from both right and left side, as shown in Fig. 1. The uniform electric and magnetic fields vary in x - y plane of uniform intensity and vary only along the direction of propagation, z axis. The lateral dimensions are assumed to be much larger than the thickness in z axis.

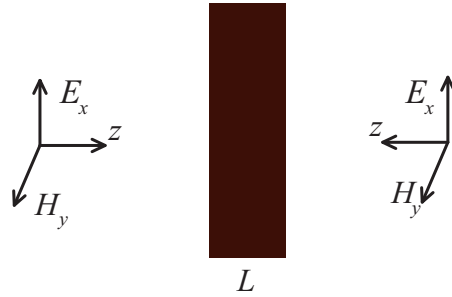


Figure 1. Physical model of microwave heating by two sources.

Microwaves heat rubber materials volumetrically, and hence, the power absorbed by the rubber due to microwave energy is included as the internal heat generation in the heat transfer equation [8]. In this paper, a one-dimensional heat transfer model is proposed to predict temperatures inside the rubber with the following assumptions:

- (1) The rubber samples are homogeneous, isotropic, and non-magnetic materials.
- (2) The mass transfer and volume changes during heating are considered negligible.
- (3) The initial temperature within samples and the section temperature at the same depth are uniform.
- (4) The rubber samples exchange heat with the outside through convection at the boundaries.
- (5) The temperature of the surrounding medium varies with the heating time.

Based on the above assumptions, the heat transfer model is expressed as follows:

$$\rho C_p \frac{\partial T(z, t)}{\partial t} = k_t \frac{\partial^2 T(z, t)}{\partial z^2} + P(z, t) \quad (1)$$

where $T(z, t)$ is the rubber sample temperature, ρ the rubber sample density, C_p the specific heat capacity at constant pressure, k_t the thermal conductivity of the rubber sample, and $P(z, t)$ the power dissipated per unit volume and can be given by the following equation [20]:

$$P(z, t) = \omega \varepsilon_0 \varepsilon''(T) \left[\frac{|A|^2}{2} e^{-2\beta(T)z} + \frac{|B|^2}{2} e^{2\beta(T)z} + |A||B| \cos(\varphi_A - \varphi_B + 2\alpha(T)z) \right], \quad 0 < z < L \quad (2)$$

where $\alpha(T)$ and $\beta(T)$ are the phase constant and attenuation constant, which depend on the dielectric constant of the rubber sample $\varepsilon'(T)$ and the dielectric loss of the rubber sample $\varepsilon''(T)$. These parameters vary with temperature. $A = |A|e^{i\varphi_A}$, $B = |B|e^{i\varphi_B}$ are the complex coefficients due to transmission and reflection, respectively. $|*|$ and φ_* are the absolute value and the argument of a complex (*). ω and ε_0 are the frequency of the incident radiation and the free space dielectric constant.

The following initial condition and boundary conditions for solving Eq. (1) are proposed:

$$\begin{aligned} T(t, z) &= T_s(t) = T_0, \quad t = 0 \\ k_t \frac{\partial T(t)}{\partial z} &= h[T(t) - T_s(t)], \quad z = 0 \\ -k_t \frac{\partial T(t)}{\partial z} &= h[T(t) - T_s(t)], \quad z = L \end{aligned} \quad (3)$$

where T_0 is the initial temperature of the rubber sample. $T_s(t)$ is the temperature of the surrounding medium, which is related to the heating time t . h is a convection heat transfer parameter.

From Eq. (2), we can find that the absorbed power is related to the phase difference of the two microwave input sources. The phase difference can be obtained either by changing the distance of the input sources or directly controlling the input phases of the input sources. Hence, the input power and the phase difference between the two input sources are regarded as control variables in the control system.

3. DESIGN OF CONTROL STRATEGIES

As the absorbed power at an arbitrary position varies with the input power and phase difference, the power distribution can be regarded as discretization actuators. The control thought of distributed sensors and actuators can be used to control microwave heating process. For actual applications, there are many influencing factors and unknown disturbances. Lyapunov-based adaptive control has good adaptability through online identification. The MTN can approximate the unknown parameters in control systems. So the adaptive MTN control law is designed by combining the adaptive control and the MTN. However, only the input powers and the phase difference between the two input sources can be controlled during the actual heating process. In order to make the power distribution equal to the calculated values, Cuckoo Search is utilized to optimize the whole situation and find the best fit inputs powers at those sampling points.

3.1. Adaptive MTN Control Law

The rubber sample is divided equally into N layers. Let's take a sample point at each interface and set the sampling period be Δt . Therefore, the control system state equation can be deduced by discretizing Eqs. (1)–(3) as

$$\mathbf{y}(k+1) = \mathbf{A}\mathbf{y}(k) + B\mathbf{u}(k) + \mathbf{D}(k) \quad (4)$$

where $\mathbf{y}(k) = [y_1(k, \Delta z), y_2(k, 2\Delta z), \dots, y_i(k, i\Delta z), \dots, y_N(k, N\Delta z)]^T$, and $y_i(k, i\Delta z)$ represents the heating sampling temperature at the k th sampling period $k\Delta t$ and the i th sampling position $i\Delta z$, $i = 1, 2, \dots, N$. $\mathbf{A}_{N \times N}$ and B are the parameter dependent on the sampling period and the thermophysical parameters of the rubber material. $\mathbf{u}(k) = [u_1(k), u_2(k), \dots, u_i(k), \dots, u_N(k)]^T$ is the

control variable. $\mathbf{D}(k) = [D_1(k, T_1), D_2(k, T_2), \dots, D_i(k, T_i), \dots, D_N(k, T_N)]^T$, where $D_i(k, T_i)$ contains the rubber sample boundary temperature that depends on surrounding temperature and the unknown conduction heat loss, and T_i is the temperature parameter at the k th sampling period and the i th sampling position.

Set the tracking error $\mathbf{e}(k) = \mathbf{y}(k) - \mathbf{y}_d(k)$, where $\mathbf{y}_d(k)$ denotes the temperature reference trajectory. The control law is designed as

$$\mathbf{u}(k) = [\mathbf{y}_d(k+1) - \mathbf{A}\mathbf{y}(k) - \mathbf{D}(\mathbf{x}(k)) - c_1\mathbf{e}(k)] \cdot B^{-1} \quad (5)$$

where $|c_1| < 1$. $\mathbf{u}(k)$ cannot be directly applied because of the unknown disturbance $\mathbf{D}(k)$. Therefore, the MTN is used to approximate the unknown disturbance. $D_i(k, T_i)$ can be approximated as

$$\hat{D}_i(k, T_i) = \hat{\theta}_i^T(k) \mathbf{P}_m(k, T_i) \quad (6)$$

where $\hat{\theta}_i(k)$ is the weight vector of the MTN. $\mathbf{P}(k, T_i) = [\underbrace{k, T_i}_{1 \text{ item}}, \underbrace{k^2, kT_i, T_i^2}_{2 \text{ item}}, \dots, \underbrace{k^m, \dots, T_i^m}_{m \text{ item}}]^T$ is the m degree polynomial function of the MTN.

Hence, for any given arbitrary approximation error bound $\varepsilon_{\max} > 0$, there exists an ideal weight vector $\theta_i^{*T}(k)$, such that [16]

$$D_i(k, T_i) = \theta_i^{*T}(k) \mathbf{P}_m(k, T_i) + \varepsilon(k, T_i) \quad (7)$$

where $\varepsilon(k, T_i)$ is the MTN inherent approximation error, $|\varepsilon(k, T_i)| \leq \varepsilon_{\max}$.

According to Eqs. (6) and (7), the MTN general approximation error is defined as

$$\tilde{D}_i(k, T_i) = \hat{D}_i(k, T_i) - D_i(k, T_i) = -\tilde{\theta}_i^T \mathbf{P}_m(k, T_i) - \varepsilon(k, T_i) \quad (8)$$

where $\tilde{\theta}_i(k) = \hat{\theta}_i(k) - \theta_i^*(k)$ denotes the weight error.

In order to design the adaptive control law that ensure system stability and tracking error convergence, a new augmented error signal is defined as

$$e_1(k-1) = \frac{\beta \left(\tilde{D}_i(k-1, T_i) - v(k) \right) - e_1(k)}{c_1} \quad (9)$$

where $v(k)$ is an auxiliary control signal, and β is a positive constant.

According to Eq. (9), the adaptive control law by Lyapunov techniques can be designed as

$$\begin{aligned} \Delta \hat{\theta}_i(k) &= \frac{\beta}{\gamma c_1^2} \mathbf{P}_m(k-1, T_i) e_1(k) & |e_1(k)| > \varepsilon_{\max}/G \\ \Delta \hat{\theta}_i(k) &= 0 & |e_1(k)| \leq \varepsilon_{\max}/G \end{aligned} \quad (10)$$

where $\Delta \hat{\theta}_i(k) = \hat{\theta}_i(k) - \hat{\theta}_i(k-1)$, γ and G are positive constants. The adaptive control process is shown in Fig. 2.

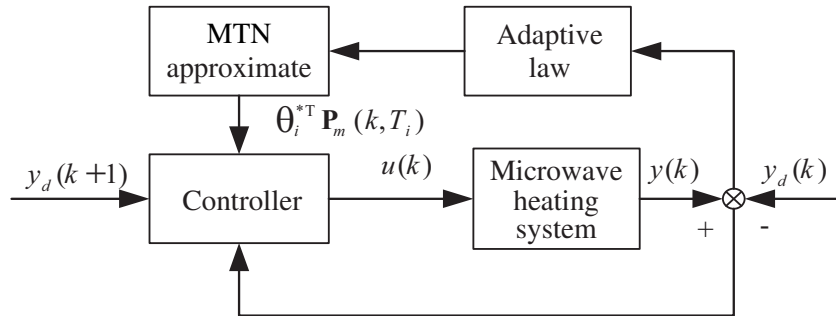


Figure 2. The adaptive control structure based on the MTN.

3.2. Stability Analysis

We assume that the control system in Eq. (4) is subjected to the control law in Eq. (5), the adaptive control law in Eq. (10), and $\|\tilde{\theta}(0)\|^2, e_1^2(0) < \infty$, where $\|\cdot\|$ denotes the Euclidean norm of a vector.

According to the adaptive control law design process, the discrete-time Lyapunov function $V(k)$ and auxiliary control signal $v(k)$ are designed as follows:

The Lyapunov function

$$V(k) = e_1^2(k) + \gamma \tilde{\theta}^T(k) \tilde{\theta}(k) \tag{11}$$

and the auxiliary signal

$$v(k) = v_1(k) + v_2(k) \tag{12}$$

where $v_1 = \frac{\beta}{2\gamma c_1^2} \mathbf{P}_m^T(k-1, T_i) \mathbf{P}_m(k-1, T_i) e_1(k)$, $v_2 = G e_1(k)$.

Then, the first-order difference of the Lyapunov function can be given:

$$\Delta V(k) = V(k) - V(k-1) = e_1^2(k) - e_1^2(k-1) + \gamma \left[\tilde{\theta}^T(k) + \tilde{\theta}^T(k-1) \right] \left[\tilde{\theta}(k) - \tilde{\theta}(k-1) \right] \tag{13}$$

Combining Eq. (9) with Eq. (13), we have

$$\begin{aligned} \Delta V(k) = e_1^2(k) - \frac{e_1^2(k) + \beta^2 \left[\tilde{D}_i(k, T_i) - v(k) \right]^2 - 2\beta \left[\tilde{D}_i(k-1, T_i) - v(k) \right] e_1(k)}{c_1^2} \\ + \gamma \left[\left(\hat{\theta}_i(k) - \theta_i^*(k) \right)^T + \left(\hat{\theta}_i(k-1) - \theta_i^*(k-1) \right)^T \right] \left[\left(\hat{\theta}_i(k) - \theta_i^*(k) \right) - \left(\hat{\theta}_i(k-1) - \theta_i^*(k-1) \right) \right] \end{aligned} \tag{14}$$

Using Eq. (8) for $\tilde{D}_i(k-1, T_i)$ and the definitions $\tilde{\theta}_i$ and $\Delta \hat{\theta}_i$, it follows that:

$$\begin{aligned} \Delta V(k) = -V_1 + \frac{2\beta \left[-\tilde{\theta}_i^T(k-1) P_m(k-1, T_i) - \varepsilon(k-1, T_i) - v(k) \right] e_1(k)}{c_1^2} \\ + \gamma \Delta \hat{\theta}_i^T(k) \Delta \hat{\theta}_i(k) + 2\gamma \tilde{\theta}_i^T(k-1) \Delta \hat{\theta}_i^T(k) \\ - V_1 + 2\tilde{\theta}_i^T(k-1) \left[\gamma \Delta \hat{\theta}_i(k) - \frac{\beta}{c_1^2} P_m(k-1, T_i) e_1(k) \right] \\ - \frac{2\beta}{c_1^2} \left[\varepsilon(k-1, T_i) + v(k) \right] e_1(k) + \gamma \Delta \hat{\theta}_i^T(k) \Delta \hat{\theta}_i(k) \end{aligned} \tag{15}$$

where

$$V_1 = \frac{e_1^2(k) (1 - c_1^2)}{c_1^2} + \frac{\beta^2 \left[\tilde{D}_i(k, T_i) - v(k) \right]^2}{c_1^2} \geq 0$$

since $0 < c_1^2 < 1$.

Substituting Eq. (10) into Eq. (15), we have

$$\Delta V(k) = \begin{cases} -V_1 - \frac{2\beta}{c_1^2} \left[\varepsilon(k-1, T_i) + v(k) \right] e_1(k) \\ + \left(\frac{\beta}{\sqrt{\gamma c_1^2}} \right)^2 \mathbf{P}_m^T(k-1, T_i) \mathbf{P}_m(k-1, T_i) e_1^2(k), & |e_1(k)| > \varepsilon_{\max}/G, \\ -V_1 - \frac{2\beta}{c_1^2} \left[\tilde{\theta}_i^T(k-1) \mathbf{P}_m(k-1, T_i) + v(k) + \varepsilon(k-1, T_i) \right] e_1(k), & |e_1(k)| \leq \varepsilon_{\max}/G. \end{cases} \tag{16}$$

Subsequently, the stability of the control system in Eq. (4) is analyzed from two aspects. On the one hand, a negative definite $\Delta V(k)$ can be obtained for $|e_1(k)| > \varepsilon_{\max}/G$ which ensures the stability of the control system in Eq. (4). On the other, when $|e_1(k)| \leq \varepsilon_{\max}/G$, for any time k , $\|\tilde{\theta}(k)\|$ and $e_1(k)$ are bounded. Moreover, the track error $e(k)$ can converge to a bound that could be predetermined by choosing appropriate design parameters. The detailed analysis of these results can be referred to Lemma 5.6.1 and Theorem 5.6.1 in [21]. Hence, the stability analysis of the control system in Eq. (4) shows that the adaptive controller proposed in this paper can achieve the boundedness of all signals as well as the convergence of the tracking errors.

3.3. Optimization Algorithm

The needed power distribution at each sampling position can be obtained by using the above control strategies. However, only the input powers and the phase difference between the two input sources can be controlled during the actual heating process. In order to make the power distribution equal to the calculated values, Cuckoo Search algorithm [22] is chosen for finding the optimal input powers and phase difference. The pseudo code of the Cuckoo Search used in this paper can be referred to [15]. The whole control system structure is shown in Fig. 3.

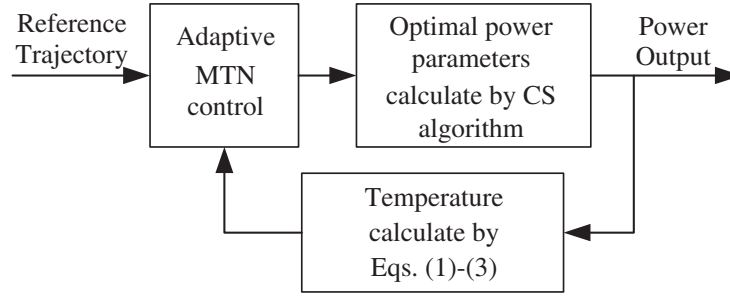


Figure 3. The control system structure block diagram.

Based on the control flow as shown in Fig. 2 and Fig. 3, a control simulation system can be designed, which mainly includes temperature measurement module, power and phase difference generation module, control module constructed by computer and programmable logic controller. Temperature sensors are employed to measure the NBR sample temperature at the sampling points. The measured data are directly transmitted to the computer, where the control method runs. Based on the measured data and reference temperature, the optimal microwave output powers and phase differences are calculated by using the control program and then sent to the programmable logic controller to lead the output power and phase difference generation.

4. EXPERIMENTAL AND SIMULATION RESULTS

To verify the effectiveness of the proposed control method, this section consists of two parts. The first part is to choose NBR composites as the rubber sample and calculate the electromagnetic parameters of the sample. Then, the proposed control method is used to get the best fit input power needed at each sampling point by considering the difference between the sampling temperature and reference trajectory.

4.1. Measurement of Complex Permittivity

The NBR composites including the common composite rubber additive are shown in Table 1. The thermophysical parameters of the sample are specific heat capacity $C_p = 1671.8 \text{ J} \cdot \text{K}^{-1} \cdot \text{kg}$, thermal conductivity $k_t = 0.25 \text{ W} \cdot \text{K}^{-1} \cdot \text{m}^{-1}$, and density $\rho = 1309.1 \text{ kg} \cdot \text{m}^{-3}$. When the microwave frequency is 915 MHz, the temperature dependent dielectric constant and dielectric loss are measured by the equipment of Novocontrol Concept 72, and the measured data are fitted to polynomials using a least-squares method as shown in Fig. 4.

The temperature dependent dielectric constant is

$$\epsilon' = -2.7768e - 06T^3 + 0.003149T^2 - 1.1551T + 141.5841$$

Table 1. The formulas of the NBR composites.

Abbreviation	NBR	S	C	CZ	SA	ZnO
Weight fraction	100	2	3	1.5	2	5

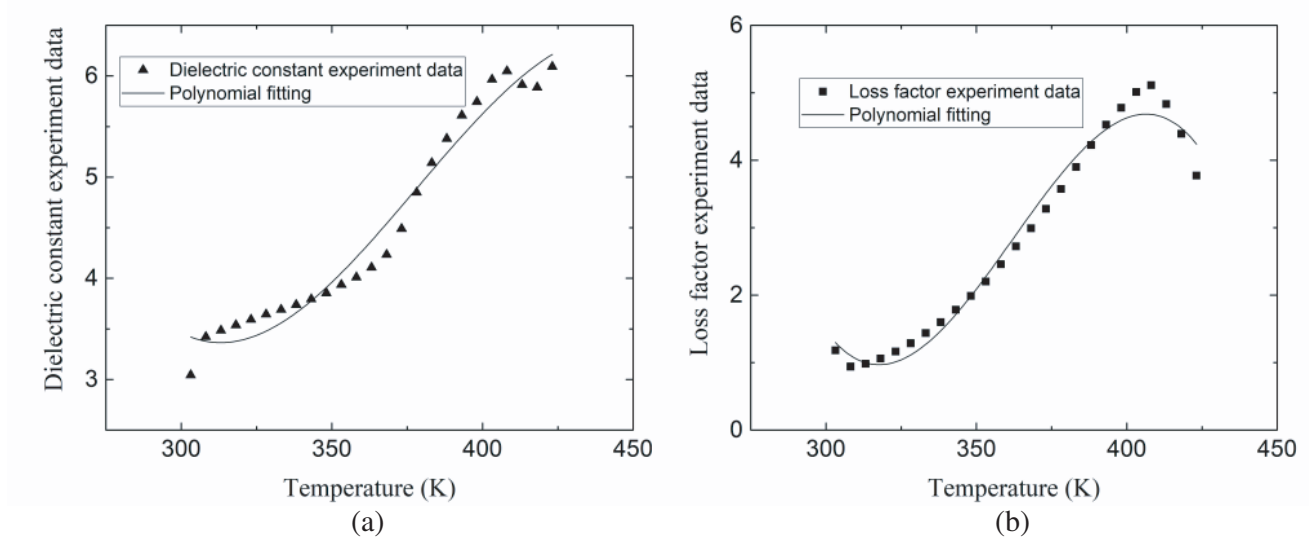


Figure 4. The temperature dependent dielectric properties: (a) Dielectric constant; (b) Dielectric loss.

and the dielectric loss is

$$\epsilon'' = -1.0605e - 05T^3 + 0.01152T^2 - 4.1071T + 483.3151$$

4.2. Simulation Results

During the heating process, the dielectric constant of the NBR sample at arbitrary position varies with temperature. The change of dielectric constant will be very small when the temperature difference under control algorithm is small. To make the simulation approximate reality, the sampling period is usually quite short. Therefore, it is assumed that the dielectric constant is the result of average temperature at each sampling period. The existing errors can be compensated by using the controller.

When the NBR sample is exposed by the microwave sources, its power distribution is related to its thickness. If the sample thickness is much larger than its penetration depth, uniform temperature field cannot be obtained during the heating process. The penetration depth is 5.54 cm for the NBR sample temperature of 290 K. So the sample with thickness less than 5.54 cm can be chosen as the object of study. Here, the thickness of the sample $L = 2$ cm is chosen. The used microwave frequency is 915 MHz. The initial temperature of the sample and environment is set as $T_0 = 290$ K. The convection heat transfer coefficient is selected empirically as $h = 2 \text{ W} \cdot \text{m}^{-2}\text{K}^{-1}$. According to the vulcanization characteristics of the NBR material, the temperature reference trajectory is set as

$$y_d = \begin{cases} T_0 + 0.7k, & 0 \leq k < 200, \\ 430, & k \geq 200. \end{cases}$$

Considering the low conductivity of the NBR material, the sample is divided equally into $N = 5$ layers, and then six sampling points are selected. To illustrate the actual feasibility of the control method, the sample period is set as $\Delta t = 1$ s, which is the same as that of the simulation experiment in [14]. The adaptive control parameters are set empirically as $c_1 = -0.01$, $\beta = 0.001$, $\gamma = 0.001$, $G = 50000$, $\epsilon_{\max} = 0.003$.

A uniform temperature distribution is obtained by the proposed control method during the heating process as shown in Fig. 5(a). At the same heating time, there is no significant difference in the temperature between different sample points. Figs. 5(b) and (c) show the average temperature tracking process and the temperature difference between the average temperature at the sampling point and the reference, respectively. From Fig. 5(b), it can be seen that the tracking process can well fit the temperature reference trajectory. At the beginning of the heating process, the MTN cannot exactly learn the internal character of the system as a result that the temperature difference is a bit large.

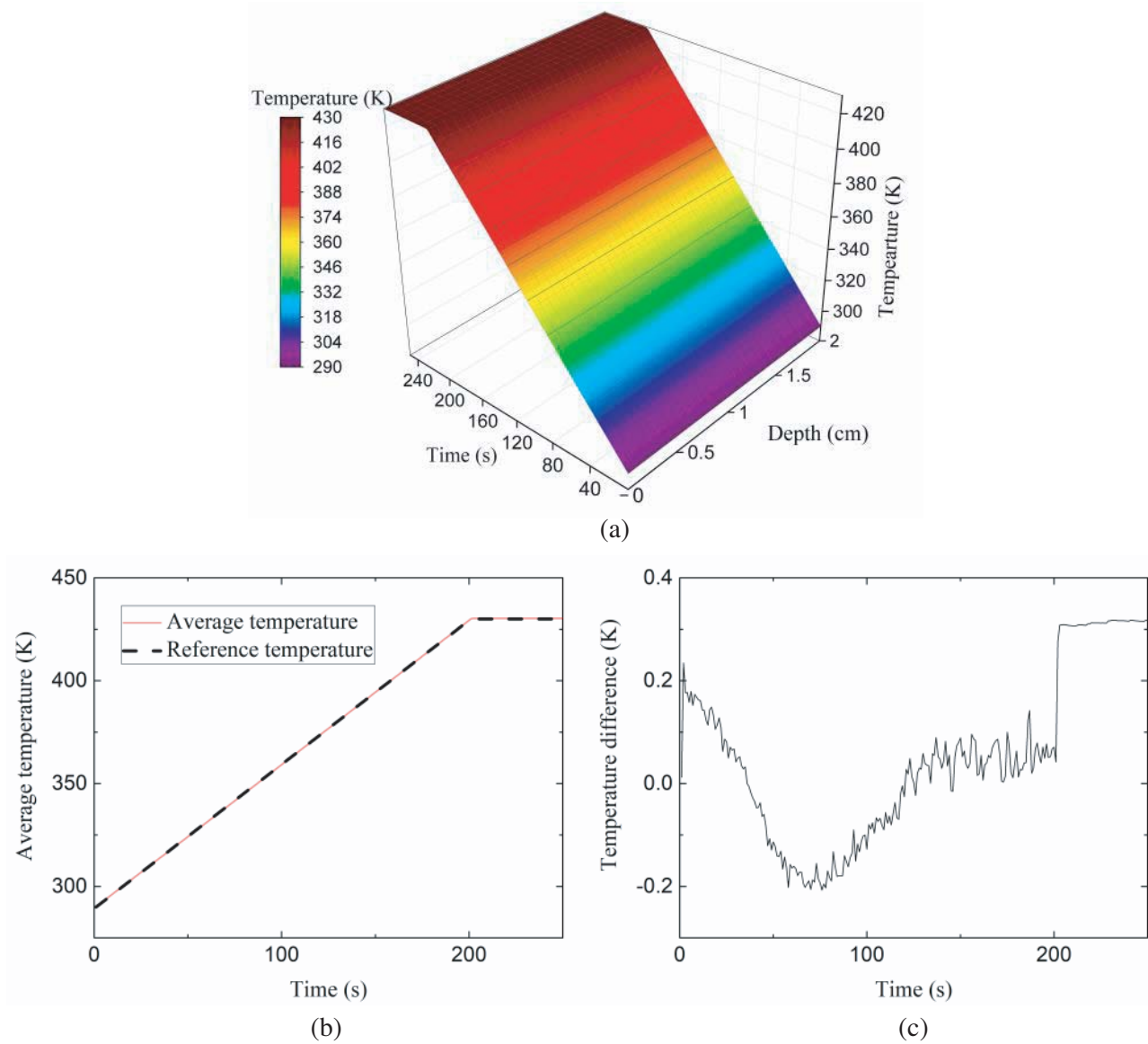


Figure 5. The NBR sample heating process: (a) Temperature rising process; (b) Average temperature tracking; (c) Temperature difference results.

With the learning of the MTN, the temperature difference decreases with heating time, which shows that good tracking performance has been achieved in a very short time. At the time about 200 s, the reference temperature suddenly jumps, but the MTN still retains the previous learning information, which results in a slightly larger temperature difference with a small overshoot. During the heating process, the temperature difference varies only from 0.3 K to -0.3 K, as shown in Fig. 5(c). From Figs. 5(a), (b), and (c), it is shown that the proposed control method has a good control effect and achieve the high tracking performance.

Figures 6(a), (b), and (c) display the variation process of two microwave output powers and the phase difference, respectively. These variation processes are consistent with those in Fig. 5. At each sampling period, since the temperature difference between each sampling point and the reference may be quite different, the powers and phase difference change a lot. The power distribution within the NBR sample will produce large nonuniform, which enlarges the temperature difference at the next control step. Therefore, in order to decrease the error, the optimal output power and phase difference

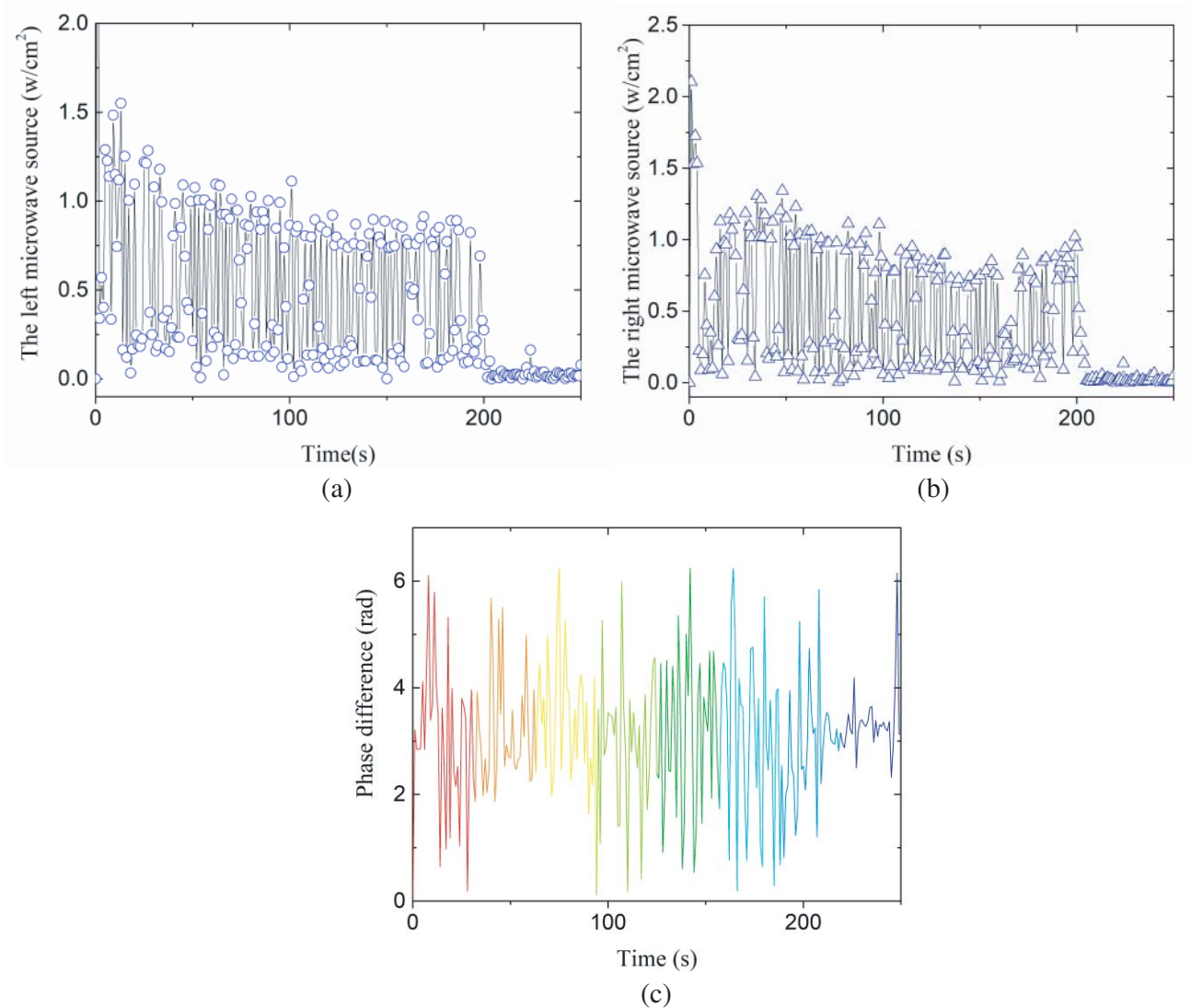


Figure 6. Two microwave sources output powers and the phase difference results: (a) Left microwave sources; (b) Right microwave sources; (c) Phase difference.

at each sampling time will change dramatically. But about 200 s later, the powers required to retain the NBR sample with the same temperature are quite small and stable owing to the constant reference temperature and the low heat loss by convective.

5. CONCLUSION

During the microwave heating process, due to uneven temperature affecting the application of microwave technology in rubber industry, it is meaningful to study the control method of temperature uniformity by using the modern control theory. In this paper, a novel control method of adaptive MTN combined with Cuckoo Search is proposed under microwave heating by two sources. The suitable output powers and phase difference are obtained by applying the adaptive MTN control method under unknown system parameters. Cuckoo Search algorithm is utilized to find the best fit inputs variables at the sampling points. The simulation results show that the difference between the average and the reference trajectory is controlled well, and the uniform temperature rising process of the sample can be realized.

ACKNOWLEDGMENT

This work was supported by Natural Science Foundation of Shandong Province (zr2019mec030), Fundamental Research Funds for the Central Universities (2242019k30017).

REFERENCES

1. Makul, N. and P. Rattanadecho, "Microwave pre-curing of natural rubber-compounding using a rectangular wave guide," *International Communications in Heat and Mass Transfer*, Vol. 37, No. 7, 914–923, 2010.
2. Keangin, P., U. Narumitbowonkul, and P. Rattanadecho, "Analysis of temperature profile and electric field in natural rubber glove due to microwave heating: Effects of waveguide position," *Conference Series: Materials Science and Engineering*, Vol. 297, No. 1, 12–37, 2018.
3. Sombatsompop, N. and C. Kumnuantip, "Comparison of physical and mechanical properties of NR/carbon black/reclaimed rubber blends vulcanized by conventional thermal and microwave irradiation methods," *Journal of Applied Polymer Science*, Vol. 100, No. 6, 5039–5048, 2006.
4. Chen, H. L., T. Li, Y. Liang, et al., "Experimental study of temperature distribution in rubber material during microwave heating and vulcanization process," *Heat and Mass Transfer*, Vol. 53, No. 3, 1051–1060, 2017.
5. Chen, H. L., T. Li, K. Li, et al., "Experimental and numerical modeling research of rubber material during microwave heating process," *Heat and Mass Transfer*, Vol. 54, No. 5, 1289–1300, 2018.
6. Chen, H. L., T. Li, K. Xing, et al., "Experimental investigation of technological conditions and temperature distribution in rubber material during microwave vulcanization process," *Journal of Thermal Analysis and Calorimetry*, Vol. 130, No. 3, 2079–2091, 2017.
7. Landini, L., S. G. Araújo, A. B. Lugão, and H. Wiebeck, "Preliminary analysis to BIIR recovery using the microwave process," *European Polymer Journal*, Vol. 43, No. 6, 2725–2731, 2007.
8. Campañone, L. A. and N. E. Zaritzky, "Mathematical analysis of microwave heating process," *Journal of Food Engineering*, Vol. 69, No. 3, 359–368, 2005.
9. Mishra, R. R. and A. K. Sharma, "Microwave-material interaction phenomena: Heating mechanisms, challenges and opportunities in material processing," *Composites Part A: Applied Science and Manufacturing*, Vol. 81, 78–91, 2016.
10. Chandrasekaran, S., S. Ramanathan, and T. Basak, "Microwave material processing — A review," *AIChE Journal*, Vol. 58, No. 2, 330–363, 2012.
11. Agrawal, D., "Latest global developments in microwave materials processing," *Materials Research Innovations*, Vol. 14, No. 1, 3–8, 2010.
12. Huang, L. H. and J. Sites, "Automatic control of a microwave heating process for in-package pasteurization of beef frankfurters," *Journal of Food Engineering*, Vol. 80, 226–233, 2007.
13. Akkari, E., S. Chevallier, and L. Boillereaux, "Global linearizing control of MIMO microwave-assisted thawing," *Control Engineering Practice*, Vol. 17, No. 1, 39–47, 2009.
14. Li, J., Q. Xiong, K. Wang, et al., "Temperature control during microwave heating process by sliding mode neural network," *Drying Technology*, Vol. 34, No. 2, 215–226, 2016.
15. Li, J., Q. Xiong, K. Wang, et al., "Combining sliding mode neural network with Cuckoo Search to make a uniform microwave heating process," *International Journal of Applied Electromagnetic and Mechanics*, Vol. 49, No. 1, 61–77, 2015.
16. Han, Y. Q. and H. S. Yan, "Adaptive multi-dimensional Taylor network tracking control for SISO uncertain stochastic non-linear systems," *IET Control Theory & Applications*, Vol. 12, No. 8, 1107–1115, 2018.
17. Yan, H. S., Y. Q. Han, and Q. M. Sun, "Optimal output-feedback tracking of SISO stochastic nonlinear systems using multi-dimensional Taylor network," *Transactions of the Institute of Measurement and Control*, Vol. 40, No. 10, 3049–3058, 2018.
18. Han, Y. Q., "Adaptive tracking control of nonlinear systems with dynamic uncertainties using neural network," *International Journal of Systems Science*, Vol. 49, No. 7, 1391–1402, 2018.

19. Yan, H. S. and A. M. Kang, "Asymptotic tracking and dynamic regulation of SISO non-linear system based on discrete multi-dimensional Taylor network," *IET Control Theory & Applications*, Vol. 11, No. 10, 1619–1626, 2017.
20. Ayappa, K. G., H. T. Davis, G. Crapiste, et al., "Microwave heating: An evaluation of power formulations," *Chemical Engineering Science*, Vol. 46, No. 4, 1005–1016, 1991.
21. Fabri, S. G. and V. Kadiramanathan, *Functional Adaptive Control: An Intelligent Systems Approach*, Springer-Verlag, London, 2001.
22. Yang, X. S. and S. Deb, "Engineering optimisation by cuckoo search," *International Journal of Mathematical Modeling and Numerical Optimisation*, Vol. 1, No. 4, 330–343, 2010.